

Learning Emergent Random Access Protocol for LEO Satellite Networks

Ju-Hyung Lee, *Member, IEEE*, Hyowoon Seo, *Member, IEEE*, Jihong Park, *Member, IEEE*, Mehdi Bennis, *Fellow, IEEE*, and Young-Chai Ko, *Senior Member, IEEE*

Abstract—A mega-constellation of low-altitude earth orbit (LEO) satellites (SATs) are envisaged to provide a global coverage SAT network in beyond fifth-generation (5G) cellular systems. LEO SAT networks exhibit extremely long link distances of many users under time-varying SAT network topology. This makes existing multiple access protocols, such as random access channel (RACH) based cellular protocol designed for fixed terrestrial network topology, ill-suited. To overcome this issue, in this paper, we propose a novel grant-free random access solution for LEO SAT networks, dubbed *emergent random access channel protocol (eRACH)*. In stark contrast to existing model-based and standardized protocols, eRACH is a model-free approach that emerges through interaction with the non-stationary network environment, using multi-agent deep reinforcement learning (MADRL). Furthermore, by exploiting known SAT orbiting patterns, eRACH does not require central coordination or additional communication across users, while training convergence is stabilized through the regular orbiting patterns. Compared to RACH, we show from various simulations that our proposed eRACH yields 54.6% higher average network throughput with around two times lower average access delay while achieving 0.989 Jain’s fairness index.

Index Terms—LEO satellite network, random access, emergent protocol learning, multi-agent deep reinforcement learning, 6G.

I. INTRODUCTION

We are at the cusp of an unprecedented revolution led by thousands of low earth orbit (LEO) satellites (SATs) in space. SpaceX has already launched more than 1,500 Starlink LEO SATs [1]–[3] covering 12 countries in 3 different continents [4]. Besides, federal communications commission (FCC) has recently authorized Amazon Project Kuiper to launch half of 3,236 LEO SATs by 2026 and the rest by 2029 [5]. The ramification of this LEO SAT mega-constellation is not only limited to advancing conventional SAT applications such as high-precision earth observation [6] but also envisaged to open up a new type of wireless connectivity, i.e., non-terrestrial networks (NTNs) in beyond the fifth-generation (5G) or 6G cellular systems [7]. While each SAT plays a role as a mobile base station (BS), a mega-constellation of LEO SATs has a great potential in provisioning fast and reliable connectivity

to ground users anywhere in the globe, including ocean, rural areas, and disaster sites [8]–[10].

Notwithstanding, each SAT BS has an extremely wide coverage (e.g., 160 – 1000 [km] inter-SAT BS distance [11]), disallowing sophisticated central coordination among SAT BSs and users in real-time under limited communication and computing resources. Furthermore, as opposed to fixed terrestrial BSs, SAT BSs move, requiring location-specific resource management. Unfortunately, existing model-based and standardized protocols, such as carrier-sense multiple access (CSMA) based WiFi protocols and random access channel (RACH) based cellular protocols, cannot flexibly optimize their operations without incurring severe protocol fragmentation, not to mention a significant effort in protocol standardization for a myriad of possible scenarios.

To overcome the aforementioned fundamental challenges in LEO SAT networks, in this article, we develop a novel model-free random access (RA) protocol that naturally emerges from a given local SAT random access environment, dubbed *emergent random access channel protocol (eRACH)*. In eRACH, the emergence of RA protocol is induced by deep reinforcement learning (DRL) at the ground user agents by utilizing locally observable information, not requiring inter-agent communication or centralized training. Consequently, eRACH jointly takes into account SAT associations and RA collision avoidance in a given local environment, thereby achieving lower RA latency and high downstream communication efficiency after eRACH.

The fundamentals of eRACH are laid by *protocol learning* via multi-agent DRL (MADRL). Several recent works have underpinned the effectiveness of protocol learning [12]–[14] in that the learned protocols can adapt to various environments while achieving higher communication efficiency than those of model-based protocols. However, these benefits come at the cost of additional inter-agent communication for MADRL, which are non-negligible under non-stationary network topologies, questioning the feasibility of protocol learning for LEO SAT networks. In fact, MADRL agents in [12]–[14] learn to communicate by exchanging local state information of each agent using a few bits, where the information exchange between agents is often referred to as a *cheap talk*. Such cheap talks may no longer be cheap under a non-stationary topology of an LEO SAT network, which may require a large amount of local state information for RA and SAT BS associations.

In this respect, our proposed eRACH is designed based on locally observable information. We extensively test which of the locally observable information candidates are essential

J.-H. Lee and Y.-C. Ko are with the School of Electrical and Computer Engineering, Korea University, Seoul 02841, Korea (e-mail: {leejuhyung, koyc}@korea.ac.kr).

J. Park is with the School of Information Technology, Deakin University, Geelong, VIC 3220, Australia (e-mail: jihong.park@{deakin.edu.au, gist.ac.kr}).

H. Seo and M. Bennis are with the Centre for Wireless Communications, University of Oulu, Oulu 90014, Finland (e-mail: {hyowoon.seo, mehdi.bennis}@oulu.fi).

on eRACH training. Surprisingly, it is shown that eRACH does not even require cheap talks. Instead, eRACH exploits 1) the expected SAT location that is known a priori owing to the pre-determined SAT orbiting pattern and 2) the collision events that are inherently observable without additional costs. While training eRACH, we have validated that the expected SAT location contains sufficient information on the network topology, as long as the variance between the expected and the actual SAT locations is less than 1 [km]. Furthermore, we have realized that the collision event contains sufficient information on how crowded each SAT BS is. Given 1) and 2), thanks to the periodic orbiting pattern of LEO SAT, the problem of MADRL frequently revisits the almost identical environment, ensuring to discover an optimal protocol carrying out SAT BS association and RA decisions.

We summarize our contributions in this paper as follows.

- We propose a novel emergent RA protocol for a ground-to-LEO SAT communication network, dubbed eRACH. To the best of our knowledge, this is the first of its kind to show that a new protocol that collaborates between multi-agents can emerge by utilizing just locally observable information, especially suited for LEO SAT networks. This is done by developing an actor-critic-based neural network architecture and a fully distributed MADRL framework without any inter-agent communication (see **Algorithm 1** in Sec. IV).
- To provide an upper-bound performance, we additionally introduce a cheap-talk inter-agent communication into eRACH, and propose a variant of eRACH, termed eRACH-Coop (see Sec. V-A).
- Numerical results corroborate that while eRACH-Coop achieves the highest average network throughput with the lowest collision rate at the cost of the cheap talk overhead, eRACH still achieves up to 6.02x and 54.6% higher average network throughput with 10x and 2x lower average RA latency than slotted ALOHA and conventional cellular RACH, respectively (see **Table II** in Sec. V).
- Furthermore, the distributed operations and the limited local information of eRACH inherently promote equal RA opportunities for all users, yielding 23.6% higher Jain's fairness than eRACH-Coop (see **Table II** in Sec. V).

The remainder of this article is organized as follows. In Sec. II, we first summarize the RA protocols for the traditional stationary SAT and for the emerging non-stationary SAT networks. In Sec. III, network model, system scenario, and performance matrices are presented. Then, the emergent contention-based RA for the LEO SAT networks, called eRACH, is proposed, which is addressed by our proposed multi-agent Actor-Critic based algorithm in Sec. IV. In Sec. V, simulation results are provided, followed by concluding remarks in Sec. VI.

Notation: Throughout this paper, we use the normal-face font to denote scalars, and boldface font to denote vectors. We use $\mathbb{R}^{D \times 1}$ to represent the D -dimensional space of real-valued vectors. We also use $\|\cdot\|$ to denote the L^2 -norm, which is a Euclidean norm, and use $(\cdot)^\dagger$ to represents conjugate transpose.

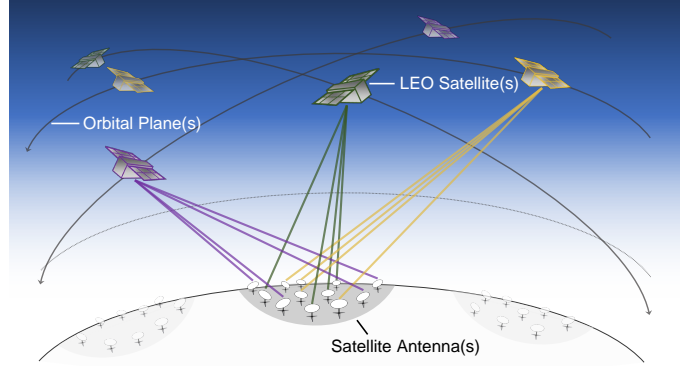


Figure 1: An illustration of random access in LEO satellite networks.

$\nabla_{\mathbf{x}} f(\mathbf{x})$ denotes the gradient vector of function $f(\mathbf{x})$, i.e., its components are the partial derivatives of $f(\mathbf{x})$. \mathbf{I}_N is the identity matrix of size N .

II. RELATED WORKS AND BACKGROUNDS

A. Random Access for Satellite Networks

In traditional SAT networks, most of the access protocols have been developed for geosynchronous equatorial orbit (GEO) SATs, also known as geostationary SATs [15]. Slotted ALOHA scheme is widely used for GEO SAT network systems owing to its simple implementation. Various types of slotted ALOHA have been further proposed, taking into account the characteristics of GEO SAT, including large propagation latency [16], [17]. However, these ALOHA-based access protocols fail to support many user terminals due to a lack of collision control. Designing multiple access protocols for SAT networks, long round trip time (RTT) latency limits the adoption of conventional access techniques, such as CSMA/CA. Such long RTT latency is induced by long one-way propagation delay in GEO SAT network (approximately 120 [ms]) and in LEO SAT network (approximately 1 - 5 [ms]). Particularly for GEO SAT networks, centralized reservation schemes are employed which avoid failed access attempts prior to the packet transmission to cope with such long RTT latency [15]. However, for LEO SAT networks which connect a myriad of scattered terrestrial user terminals, the coordinated method requires a significant system overhead.

In contrast to stationary GEO SAT networks, emerging LEO SAT networks, wherein numerous LEO SATs orbit rapidly at a speed of around 7.6 [km/s] (see Fig. 1), are dynamic and require frequent and fast handovers [18], [19], calling for another channel access considering not only long RTT latency but also the inherent dynamics of LEO SAT networks. In this regard, the contention-based random access channel (RACH), adopted for cellular networks (e.g., 5G NR, 4G LTE/LTE-A), is also considered for LEO SAT networks [20], [21]. The contention-based RACH procedure is used to initialize and synchronize prior to allocating resources in downlink (DL) and uplink (UL) channels. In the RACH, a sender randomly transmits short packet preambles to the receiver and then waits for a positive response from the receiver prior to transmitting the complete message. Particularly, the RACH protocol is initiated by transmission of a randomly chosen

preamble through physical RACH (PRACH) for the preamble transmission. The basic RACH is designed to follow the four-step message exchanging procedure, that is, 1) PRACH transmission, 2) random access response (RAR), 3) radio resource control (RRC) connection request, and 4) an RRC connection setup (and resolution). By the four-step procedure and utilizing Zadoff-Chu (ZC) sequences, RACH is able to control collision events while attempting to access many users. Despite this, RACH is not ideally suited for LEO SAT networks as it does not take into account SAT associations [22], [23]. As such, existing access protocols have some limitations for non-stationary LEO SAT networks.

To design LEO SAT-oriented access protocol, we need to consider the following two conditions: 1) Collisions need to be managed efficiently without centralized access control; and 2) SAT associations and backoff mechanisms need to be jointly optimized to achieve low access delay and high spectral efficiency. The current standardized protocols and archetypical model-based algorithms face several challenges, mainly due to the non-stationarity of the LEO SAT network topology. Recently, a model-free protocol has been studied in the context of emergent communication, using model-free DRL algorithms, e.g., Actor-Critic [24], Q -learning [25], and deep deterministic policy gradient (DDPG) [26], which can be an alternative solution for the time-varying network topology.

B. Emergence of Protocol through MADRL

Pioneered by [12], [27], the topic of emergent communication has arisen firstly in the deep learning literature. In [12], Foerster et al. studied how languages emerge and how to teach natural languages to artificial agents. Spurred by this trend of emergent communication, Hoydis et al. adopted the idea of emergent communication into cellular systems in [13], [14]. Here, MAC signaling is interpreted as a language spoken by the user equipment (UE) and the base station (BS) to coordinate while pursuing the goal of delivering traffic across a network. Therein, two distinct policies (i.e., a channel access policy and a signaling policy) are trained by using the off-the-shelf learning-to-communicate (L2C) techniques (e.g., DIAL and RIAL in [12]). This approach has shown the potential of the emergent protocol design in their particular scenario.

Despite the novelty of [13], [14], the superior performance of the learned protocol largely depends on the learning of cheap-talk exchanged between network nodes, which incurs additional communication and learning overhead. Moreover, the proposed method assumes centralized training that requires each network node to obtain full-observable information; it is an obstacle to actual system application. Besides, in these works, the protocol was optimized for only stationary networks. Thus, it is still questionable whether a protocol for non-stationary networks can emerge without relying too much on information exchange between agents.

III. SYSTEM MODEL

A. Network and Channel Models

Consider a set \mathcal{K} of orbital planes around the earth, sets \mathcal{I}_k of LEO SATs orbiting on the orbital plane k for all $k \in \mathcal{K}$, and

a set \mathcal{J} of SAT user terminals (UTs) deployed on the ground inside an area A . The position of UT $j \in \mathcal{J}$ is expressed as a 3-dimensional real vector on Cartesian coordinates denoted by $\mathbf{q}_j = (q_j^x, q_j^y, q_j^z) \in \mathbb{R}^3$, and similarly, the position and velocity of SAT $i \in \bigcup_{k \in \mathcal{K}} \mathcal{I}_k$ at time $t \geq 0$ is denoted by $\mathbf{q}_i(t) = (q_i^x(t), q_i^y(t), q_i^z(t)) \in \mathbb{R}^3$ and $\mathbf{v}_i(t) = (v_i^x(t), v_i^y(t), v_i^z(t)) \in \mathbb{R}^3$, respectively, for all $i \in \bigcup_{k \in \mathcal{K}} \mathcal{I}_k$. Suppose the number of SATs on each orbital plane is equal to each other given as $|\mathcal{I}_k| = I$ for all $k \in \mathcal{K}$, and assume all SATs are moving in uniform circular motion with the same orbital period T , while the arc length between any two neighboring SATs on the same orbital plane is equal to each other.

Consider that time is discretized in slots of length τ and let $\mathbf{q}_i[0]$ be the initial position of the SAT $i \in \bigcup_{k \in \mathcal{K}} \mathcal{I}_k$ at time $t = 0$. Then, by following the discrete-time state-space model [19], [28], the position of SAT i at time $t = m\tau$ can be expressed as

$$\mathbf{q}_i(m\tau) \approx \mathbf{q}_i(0) + \tau \sum_{m'=1}^m \mathbf{v}_i(m'\tau) + \mathbf{n}_i, \quad (1)$$

where \mathbf{n}_i is the additive random noise representing the perturbation on the i -th satellite position and attitude determination error [29], whose entries are independent and identically distributed zero-mean Gaussian random variables with $\mathbb{E}[\mathbf{n}_i \mathbf{n}_i^\dagger] = \sigma_i^2 \mathbf{I}_3$.

Communication channels between SATs and UTs follow the characteristics of ground-to-space (or space-to-ground) RF link [30]. The channel gain between satellite $i \in \bigcup_{k \in \mathcal{K}} \mathcal{I}_k$ and UT $j \in \mathcal{J}$ at time t is expressed as

$$h_{i,j}(t) = \tilde{h}_{i,j}(t) \sqrt{\gamma_{i,j}(t)}, \quad (2)$$

where $\gamma_{i,j}(t)$ and $\tilde{h}_{i,j}(t)$ are the effects of large-scale (e.g., path loss and shadowing) and small-scale fading at time t , respectively, and $\mathbb{E}[|\tilde{h}_{i,j}(t)|^2] = 1$ for all $t \geq 0$.

The large-scale fading is modeled based on the tractable line-of-sight (LoS) probability model [30], [31] with shadowing and blockage effects. Note that in the LoS probability model, the large-scale fading follows generalized Bernoulli distribution of two different events; the channel is LoS or non-LoS (NLoS) with a certain probability. The probability of event that a channel between SAT i and UT j at time t being LoS is modeled as

$$\varphi_{i,j}^{\text{LoS}}(t) = \frac{1}{1 + L_1 \exp[-L_2(\theta_{i,j}(t) - L_1)]}, \quad (3)$$

where L_1 and L_2 are the environmental parameters depending on the propagation condition [32] and

$$\theta_{i,j}(t) = \frac{180}{\pi} \sin^{-1} \left(\frac{q_i^z(t) - q_j^z}{\|\mathbf{q}_i(t) - \mathbf{q}_j\|_2} \right) \quad (4)$$

is the angle of SAT i and UT j referred to as an elevation angle.

Meanwhile, depending on whether the channel is LoS or NLoS, different large-scale fading $\gamma_{i,j}(t)$ can be expressed as

$$\gamma_{i,j}(t) = \begin{cases} \beta_o \|\mathbf{q}_i(t) - \mathbf{q}_j\|_2^{-\alpha}, & \text{for LoS channel,} \\ \kappa \beta_o \|\mathbf{q}_i(t) - \mathbf{q}_j\|_2^{-\alpha}, & \text{for NLoS channel,} \end{cases} \quad (5)$$

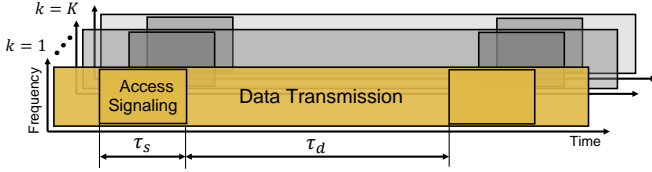


Figure 2: Time and frequency resource structure of the considering random access scenario.

where β_o is the average power gain at the reference distance $d_o = 1$ [m], α is the path loss exponent and κ is the attenuation scaling factor in the NLoS link [31]. Note that $\tilde{h}_{i_k,j}$ has its randomness from both random occurrence of LoS and NLoS as well as the small-scale fading. Accordingly, the expected channel gain over both randomness is given by

$$\mathbb{E}[|h_{i,j}(t)|^2] = \tilde{\varphi}_{i,j}^{\text{LoS}}(t)\beta_o\|\mathbf{q}_i(t) - \mathbf{q}_j\|_2^{-\alpha}, \quad (6)$$

where $\tilde{\varphi}_{i,j}^{\text{LoS}}(t) = \varphi_{i,j}^{\text{LoS}}(t) + \kappa(1 - \varphi_{i,j}^{\text{LoS}}(t))$.

B. LEO SAT Random Access Scenario

Consider an LEO satellite random access (RA) scenario, where UTs attempt to access to LEO satellite networks for radio resource grant. Suppose that UTs always have data to transmit in their infinite length queue, and thus, they always have intentions to RA at every opportunity they have. Each UT has information of the periodic position of SATs on each orbital plane and attempts to access only to the closest SAT on each orbital plane. For the sake of convenience, we assume that the closest SAT on each orbital plane is the same for every UT at the same time point. According to the network model, note that the time duration that one SAT becomes the closest among all SAT on each orbital plane is $\frac{T}{I}$, where T is the orbiting period and I is the number of SATs on each orbital plane. Suppose that there are N RA opportunities during the interval $\frac{T}{I}$ and they are synchronized over all orbital planes as shown in Fig. 2. The time duration of each RA opportunity is $\frac{T}{IN}$, which incorporates RA signaling duration τ_s and data transmission duration τ_d , i.e., $\tau_s + \tau_d = \frac{T}{IN}$, for some τ_s and τ_d such that $\tau_s/\tau, \tau_d/\tau \in \mathbb{Z}^+$. For simple description, we focus only on N RA opportunities in the rest of this section and suppose the first opportunity starts at $t = 0$. Here, the time duration of each n -th RA opportunity is discretized with τ , i.e., $t = n\tau, \forall n \in \{1, 2, \dots, N\}$.

At each RA opportunity, each UT chooses whether to access or backoff, and then further decide the SAT to which it will access. Such set of actions is simply denoted by $\{\text{BACKOFF}, 1, \dots, K\}$ in which $K := |\mathcal{K}|$ is the number of orbital planes. The RA action of UT $j \in \mathcal{J}$ at RA opportunity n is denoted by

$$a_j[n] \in \{\text{BACKOFF}, 1, \dots, K\}. \quad (7)$$

Note that $a_j[n] = \text{BACKOFF}$ means that the UT j does not access at the n -th opportunity and waits for the next one. Moreover, those who attempt to access additionally choose a preamble uniform-randomly, that is

$$p_j[n] \in \{1, 2, \dots, P\}. \quad (8)$$

Here, each preamble is associated with P resources that the SATs can grant during the data transmission duration.

The RA signaling is done in two steps. First, those UTs that determine to access send preambles to the corresponding SATs. Secondly, SATs send feedback to confirm whether there were collisions or not for each chosen preamble. UTs that have chosen collided preambles fail to access, while those of UTs that have chosen preambles without collision succeed to access.

C. Collision Rate, Access Delay, and Network Throughput

The performance of RA in LEO SAT network is evaluated with collision rate, access delay and average network throughput, as explained in the following.

1) *Collision Rate*: Denote the collision indicator of UT $j \in \mathcal{J}$'s RA at opportunity $n \in \{1, \dots, N\}$ by $c_j[n]$, and define it as

$$c_j[n] = \begin{cases} 0, & (a_j[n], p_j[n]) \neq (a_{j'}[n], p_{j'}[n]) \quad \forall j' \in \mathcal{J} \setminus j \\ 1, & \text{otherwise,} \end{cases} \quad (9)$$

if $a_j[n] \neq \text{BACKOFF}$, and otherwise we have $c_j[n] = 0$. Then, the *collision rate* is defined as:

$$C = \frac{1}{|\mathcal{J}|} \sum_{n=1}^N \sum_{j \in \mathcal{J}} c_j[n]. \quad (10)$$

2) *Access Delay*: Define the access indicator of UT $j \in \mathcal{J}$'s RA at opportunity $n \in \{1, \dots, N\}$ as

$$\eta_j[n] = \begin{cases} (1 - c_j[n]), & a_j[n] \neq \text{BACKOFF} \\ 0, & a_j[n] = \text{BACKOFF} \end{cases}. \quad (11)$$

Let N_s be the number of successful accesses of all UTs out of N access attempts, which is given as

$$N_a = \frac{1}{|\mathcal{J}|} \sum_{n=1}^N \sum_{j \in \mathcal{J}} \eta_j[n]. \quad (12)$$

Then, the *average access delay* is given as:

$$D = \frac{(N_a - N)(m_s + m_d)\tau}{N_a} + m_s\tau. \quad (13)$$

3) *Network Throughput*: According to the defined channel model, the uplink (UL) throughput from UT $j \in \mathcal{J}$ to SAT $i \in \bigcup_{k \in \mathcal{K}} \mathcal{I}_k$ can be expressed as

$$R_{i,j}(t) = B \log_2 \left(1 + \frac{\Gamma |h_{i,j}(t)|^2}{\sigma_n^2} \right) [\text{bps}], \quad (14)$$

where B represent the bandwidth, σ_n^2 is the noise variance, and Γ is the UL transmission power.

Note that UT can transmit data only when its access is successful. Thus, when $a_j[n] \neq \text{BACKOFF}$, the attainable throughput at UT $j \in \mathcal{J}$ in the n -th RA opportunity can be expressed as

$$R_j[n] = \eta_j[n]\tau_d \sum_{t=(n-1)(\tau_s+\tau_d)}^{n(\tau_s+\tau_d)} R_{i_{a_j[n]},j}(t), \quad (15)$$

where $i_k \in \mathcal{I}_k$ denotes the most closest SAT from UT j among all SATs on the orbital plane $k \in \mathcal{K}$. Otherwise if $a_j[n] = \text{BACKOFF}$, $R_j[n] = 0$. Consequently, the time-average network throughput R within N RA opportunities can be given as

$$R = \frac{1}{N} \sum_{n=1}^N \sum_{j \in \mathcal{J}} R_j[n]. \quad (16)$$

In what follows, under the LEO SAT RA scenario and with the performance metrics including collision rate, access delay, and network throughput, we propose an emergent RA protocol for LEO SAT networks.

IV. EMERGENT RANDOM ACCESS PROTOCOL FOR LEO SATELLITE NETWORKS

This section introduces the emergent contention-based RA protocol for LEO SAT networks. Moreover, we explain step-by-step how the protocol is specifically designed.

A. Emergent RA Protocol for LEO SAT

We propose a novel RA solution for LEO SAT networks, coined *emergent random access channel protocol (eRACH)*. As illustrated in Fig. 1, the UT on the ground attempts to access an SAT by the contention-based RA and then transmits a data frame only when it successfully accesses to intended LEO SAT. To specifically discuss and evaluate our proposed eRACH protocol, the following optimization problem is mathematically formulated. This problem aims to maximize the throughput while minimizing the collision rate under the constraints related to the practical conditions of LEO SAT networks:

$$\begin{aligned} \max_{a_j[n]} \quad & \sum_{n=1}^N R_j[n] - \rho c_j[n], \quad \forall j \in \mathcal{J}, \\ \text{s.t.} \quad & (1), (9), \end{aligned} \quad (17)$$

where ρ denotes a normalization coefficient, which strikes a balance between throughput and collision rate, and N represents one orbital cycle of SAT. Here, the constraint in (1) represents the orbital motion of the LEO SAT constellation. Besides, the constraint in (9) represents the collision in LEO SAT. Recall that the collision occurs for UT agents that attempt to access the same LEO SAT i_k with the same preamble signature, at the same time slot.

In a nutshell, eRACH considers the following steps:

- 1) Association decision for SAT-UT,
- 2) Backoff decision,
- 3) RACH access (PRACH preamble p is chosen uniformly-randomly), and
- 4) UL data transmission (only when accessed successfully),

during which, eRACH determines 1) and 2), while the rest are automatically determined according to the established protocol as described in Sec. III-B. As 3) and 4) follow the standard operations, the problem of interest focuses on the joint decision on 1) and 2). However, to optimize 1) and 2) for (17), traditional convex optimization methods (e.g., SCA

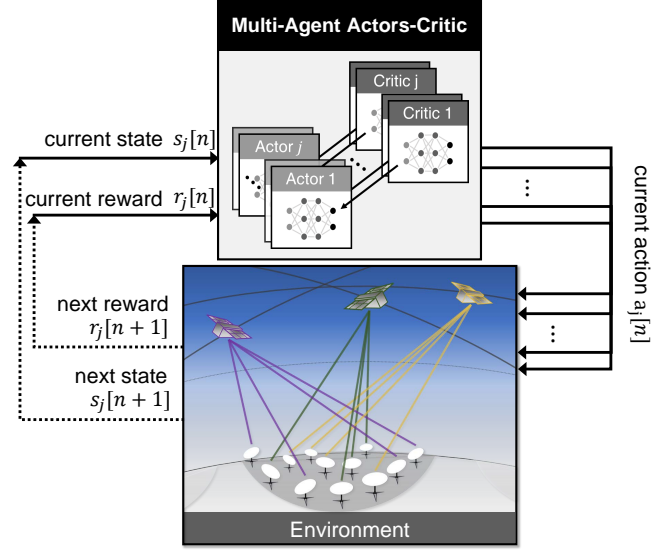


Figure 3: An illustration of the proposed eRACH training process based on multi-agent Actor-Critic method.

[33], BCD [34]) face several challenges mainly due to time-varying LEO SAT networks.

To this end, we utilize MADRL algorithm in the eRACH protocol. While training the MADRL, we only use locally observable information of UT in the LEO SAT networks. Further, considering the specificity of the LEO SAT networks, we carefully pick out a piece of essential by extensively testing candidates among locally observable information to minimize the complexity while retaining near-optimality. For applying the MADRL method, first and foremost, it is necessary to design Markov decision process (MDP) model, which includes a state, action, and reward function in an environment that reflects our network scenario, which is discussed next.

B. MADRL Formulation for Emergent RA Protocol

In what follows, we first reformulate the problem (17) of eRACH using an MDP model, and then describe how to solve this problem via MADRL.

1) *MDP Modeling*: To recast (17) as an MADRL problem, we model the SAT network scenario using an MDP, a discrete-time stochastic control process that mathematically characterizes decision-making in a random environment. In the MDP model, for a given state, a policy π refers to the probability of choosing an action, and π^* is the optimal policy maximizing the long-term average reward, which is the goal of MADRL.

Environment. As illustrated in Fig. 3, the MADRL framework under study consists of multiple UTs interacting with an environment that follows an MDP model. At each time t , each UT j is an agent observing a state $s_j[n] \in \mathcal{S}$, and takes an action $a_j[n] \in \mathcal{A}$ based on a state-action policy π . Given this action, the state of the agent j transitions from $s_j[n]$ to $s_j[n+1]$, and in return receives a reward $r_j[n]$ that reinforces the agent follows an optimal policy π^* . How to define these states, actions, and rewards significantly affects the performance, communication, and computing costs of eRACH as we shall elaborate next.

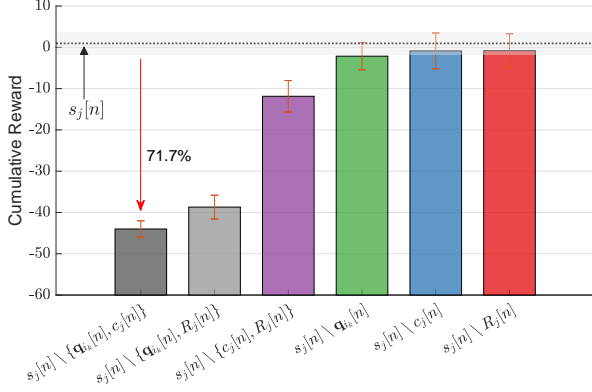


Figure 4: Comparison of cumulative rewards with different information included in the state $s_j[n]$.

State. In the aforementioned MDP model, we consider the following state of UT j :

$$s_j[n] = \{n, \mathbf{q}_{i_1}[n], \dots, \mathbf{q}_{i_K}[n], R_j[n], c_j[n], a_j[n-1]\}, \quad (18)$$

where $\mathbf{q}_{i_k}[n] \in \mathbb{R}^{I \times 3}$, $i \in \mathcal{I}$, $k \in \mathcal{K}$ denotes the position of SAT i in the orbital plane k , $R_j[n]$ is the throughput, $c_j[n]$ is a binary indicator function of an RA collision event, and $a_j[0]$ and $s_j[1]$ are initial values chosen randomly at the beginning of Algorithm 1. Here, the previous action $a_j[n-1]$ and current time slot n are used as a *fingerprint*, adopting the fingerprint-based method proposed in [35] to stabilize experience replay in the MADRL. Note that the non-stationarity of the multi-agent environment is dealt with by the fingerprinting that disambiguates the age of training samples and stabilizes the replay memory.

The state of an agent should contain sufficient information for carrying out decision-making. Meanwhile such information should be minimal to reduce any additional data collection overhead from the environment or other agents and to promote MADRL training convergence. To screen for important information to be included in the state among locally observable information, we extensively test possible local information candidates and their impacts on eRACH performance. In this regard, we provide an ablation study of Fig. 4 which presents the contribution of each information to the overall system. Each information in $s_j[n]$ has a different importance. As shown in this figure, eRACH mainly exploits the following information: 1) the expected SAT locations that are known a priori owing to the pre-determined LEO SAT orbiting pattern; and 2) the collision that are inherently observable. Such two locally observable information significantly contributes to the training of eRACH, which highlights eRACH does not even require cheap talks between agents.

While training eRACH, we validate that the expected SAT location contains sufficient information on the network topology, as long as the variance between the expected and actual SAT position is less than 1 [km] as shown in Fig. 5. Moreover, it is confirmed that the collision event incorporates sufficient information on the local environment, e.g., how crowded the network is, as will be elaborated in Sec V. As

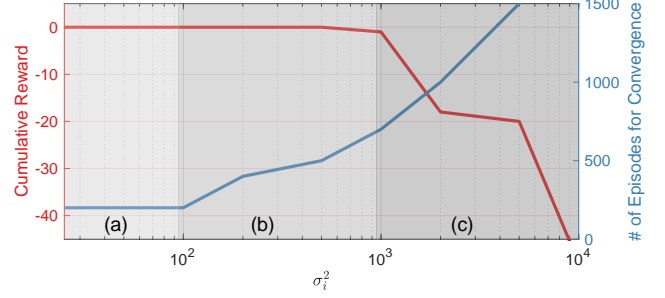


Figure 5: Robustness to SAT BS positioning errors, where shaded regions identifies the three different regimes: (a) same reward and convergence speed, (b) same reward, slower convergence, and (c) lower reward, slower convergence. Specific reward values and convergence times are reported in Table IV.

the LEO SAT periodically orbits a pre-designed trajectory, MADRL frequently revisits the same environment of SAT-UT RA, which facilitates the discovery of emergency protocols that perform SAT-UT connections and RA decisions without communication overhead between agents.

Action. The action space \mathcal{A} in our environment is related to RA. Among SATs i_k in orbital plane k , the agent UT j chooses one SAT to access by using the access action $a_j[n]$ in (7). For the set of access action, \mathcal{A} , we define an one-hot encoded action as follows

$$\mathbf{a}_j[n] = \{a_0, a_1, a_2, \dots, a_K\}, \text{ s.t. } \sum_{\ell=0}^K a_\ell = 1, \quad (19)$$

where a_ℓ for $\ell \neq 0$ denotes the association with the ℓ -th orbital plane, and a_0 implies backoff. Note that it is assumed that the UT attempts to access the nearest SAT among SATs \mathcal{I}_k in orbital plane k .

Reward. Our reward function is supposed to reinforce UTs to carry out optimal access actions that maximize the network throughput while penalizing access collision. The objective function (17) captures this goal, although it is not suitable for the reward function. Indeed, if there is no collision, (17) gives positive throughput without penalty, and otherwise imposes only collision penalty with zero throughput. This incurs too significant and frequent reward variation, hindering the training convergence. To mitigate this issue, following [25], [36], we normalize (17), and consider the reward function of UT j as follows

$$r_j[n] = g(R_j[n] - \rho c_j[n]). \quad (20)$$

Note that the normalization function is given by $g(Y) = \frac{Y-\mu}{\Sigma}$, where Σ and μ are parameters for scale which shrinks the output value Y between -1 and 1 and for mean value, respectively. Here, the mean value corresponds with the network throughput of the RACH baseline in Sec. V.

It is worth noting that the state and reward of each UT agent are all locally observable information and thus the MDP model for RA protocol can be trained and executed in a fully *distributed* manner.

2) *Actor-Critic MADRL*: Following the standard RL settings, the aforementioned SAT-UT RA environment is considered in which many agents interact for a given number of discrete time steps. At each time step n , the agent j receives a state $\mathbf{s}_j[n]$ and selects an action $\mathbf{a}_j[n]$ from some set of possible actions \mathcal{A} according to its policy π_{θ_j} , where π_{θ_j} is a mapping from states $\mathbf{s}_j[n]$ to actions $\mathbf{s}_j[n]$. In return, the agent receives the next state $\mathbf{s}_j[n+1]$ and receives a scalar reward $r_j[n]$. The process continues until the agent reaches a terminal state after which the process restarts. The return $\tilde{r}_j[n] = \sum_{k=0}^{\infty} \gamma^k r_j[n+k]$ is the total accumulated return from time step n with discount factor $\gamma \in (0, 1]$.

For our multi-agent scenario, we employ an Actor-Critic RL framework [37], which combines the benefits of both policy gradient and value-based methods. The Actor-Critic framework comprises a pair of two NNs: an Actor NN seeks to take actions to obtain higher rewards based on the policy gradient method; and its paired Critic NN aims to approximate value functions more accurately via the value-based method. In particular, each UT agent j has an Actor NN and a Critic NN and follows the synchronous advantage Actor-Critic operation [24], [37], in which the Critic NN updates its model parameters ϕ_j according to the policy π_{θ_j} given by the Actor NN. Meanwhile, the Actor NN updates its model parameters θ_j according to the value functions $V^{\pi_{\theta_j}}(\mathbf{s}_j[n]; \phi_j)$ approximated by the Critic NN. Specifically, the Critic NN aims to minimize the loss function

$$L_{\text{Critic}}^j(\phi_j) = \kappa_j [n]^2, \quad (21)$$

where $\kappa \mathbf{s}_j[n] = r_j[n+1] + \gamma V^{\pi_{\theta_j}}(\mathbf{s}_j[n+1]; \phi_j) - V^{\pi_{\theta_j}}(\mathbf{s}_j[n]; \phi_j)$ is referred to as the advantage of an action [38]. The Critic NN model parameters are then updated as

$$d\phi_j \leftarrow d\phi_j + \beta_c (R - V^{\pi_{\theta_j}}(\mathbf{s}_j[n]; \theta_j)) \nabla_{\phi_j} V^{\pi_{\theta_j}}(\mathbf{s}_j[n]; \phi_j), \quad (22)$$

where β_c is the hyperparameter of Critic NN, which is related to the value estimate loss. Meanwhile, the Actor NN aims to minimize the loss function

$$L_{\text{Actor}}^j(\theta_j) = -\kappa_j [n] \log \pi(\mathbf{s}_j[n] | \mathbf{s}_j[n]; \theta_j). \quad (23)$$

Hereafter, the index j identifies different actors for multi-agent scenarios, which can be omitted for a single agent case. Consequently, the Actor NN model parameters are updated as

$$d\theta_j \leftarrow d\theta_j + \nabla_{\theta_j} \log \pi(\mathbf{s}_j[n] | \mathbf{s}_j[n]; \theta_j) (R - V^{\pi_{\theta_j}}(\mathbf{s}_j[n]; \theta_j)). \quad (24)$$

where $H(\pi)$ is the entropy of the policy and β_e is the hyperparameter of controlling the relative contributions of the entropy regularization term. The NN parameters are updated via gradient descent and backpropagation through time, using Advantage Actor-Critic as detailed by [24]. We summarize the eRACH training process for each UT agent j in Algorithm 1.

V. NUMERICAL EVALUATIONS

This section validates the proposed emergent RA methods of eRACH for LEO SAT networks with respect to average throughput, collision rate, and delay.

Algorithm 1 eRACH Training Algorithm

```

Initialize step counter  $n \leftarrow 1$ 
Initialize episode counter  $E \leftarrow 1$ 
repeat
  Reset gradients:  $d\theta_j \leftarrow 0$  and  $d\phi_j \leftarrow 0$ 
   $n_{\text{start}} = n$ 
  Get state  $\mathbf{s}_j[n]$ 
  repeat
    Perform access action  $\mathbf{s}_j[n]$  according to policy
     $\pi(\mathbf{s}_j[n] | \mathbf{s}_j[n]; \theta_j)$ 
    Receive reward  $r_j[n]$  and new state  $\mathbf{s}_j[n+1]$ 
     $n \leftarrow n+1$ 
  until terminal  $\mathbf{s}_j[n]$ ;
   $R = \begin{cases} 0, & \text{for terminal } \mathbf{s}_j[n] \\ V^{\pi_{\theta_j}}(\mathbf{s}_j[n]; \theta_j), & \text{for non-terminal } \mathbf{s}_j[n] \end{cases}$ 
  for  $i \in \{n-1, \dots, n_{\text{start}}\}$  do
     $R \leftarrow r_j[n] + \gamma R$ 
    Accumulate gradients w.r.t.  $\theta_j$ :
     $d\theta_j \leftarrow d\theta_j + \nabla_{\theta_j} \log \pi(\mathbf{a}_j[i] | \mathbf{s}_j[i]; \theta_j) (R - V^{\pi_{\theta_j}}(\mathbf{s}_j[i]; \theta_j))$ 
     $+ \beta_e \partial H(\pi(\mathbf{a}_j[i] | \mathbf{s}_j[i]; \theta_j)) / \partial \theta$ 
    Accumulate gradients w.r.t.  $\phi_j$ :
     $d\phi_j \leftarrow d\phi_j + \beta_c (R - V^{\pi_{\theta_j}}(\mathbf{s}_j[i]; \theta_j)) \nabla_{\phi_j} V^{\pi_{\theta_j}}(\mathbf{s}_j[i]; \phi_j)$ 
  end
  Perform update of  $\theta_j$  using  $d\theta_j$  and of  $d\phi_j$  using  $d\phi_j$ 
   $E \leftarrow E + 1$ 
until  $E > E_{\text{max}}$ ;

```

Table I: Simulation parameters.

Parameter	Value
Altitude of SAT	$H_L = 550$ [km] (from [3])
Velocity (Speed) of SAT1 ($k = 1$)	$\mathbf{v}_{L,1}^1 = [0, 7590, 0]^T$ (7590 [m/s])
Velocity of SAT2 ($k = 2$)	$\mathbf{v}_{L,1}^2 = [0, -7590, 0]^T$
Radius of an orbit	$r_E = 6921$ [km]
Circumference of an orbital lane	$c_E = 43486$ [km]
Number of SATs per orbital lane	$I = 22$
Inter-SAT distance	1977 [km]
Number of UT	$J = 5$
Bandwidth	$B = 10^8$ [Hz]
Path loss exponent	$\tilde{\alpha} = 2.1$
Parameter for LoS probability	$L_1 = 10, L_2 = 0.6$
Attenuation factor	$\kappa = 0.2$
Random access duration	$\tau_s = 10$ [ms]
Data transmission duration	$\tau_d = 90$ [ms]
Preamble signatures for each SAT	$P = 2 - 54$
Orbital period	$T = 5728$ [s]
Number of time slots per episode	$N = 2604$

A. Simulation Settings

Unless otherwise stated, UTs under study are located in the ground uniformly at random within an area of 1000×1000 [m²], while two orbital planes $K = 2$ circulate over UTs at the altitude of 550 [km]. Each orbital lane consists of 22 SATs with the orbital lane circumference of 43486 [km], resulting in an inter-SAT distance of 1977 [km]. Since the orbital lane circumference is much larger than the area of interest, each orbital lane is approximated as a line segment at the altitude of 550 [km] [3], in which 22 SATs orbit with the orbital speed 7.59 [km/s], are separated with the inter-SAT distance 1977 [km], and perturbed with σ_i . Here, the orbital period and speed are calculated using the relations $4\pi^2(r_E)^3 = T^2 GM$ and $V^2 r_E = GM$, respectively, where r_E is the radius of orbit in metres; T , the orbital period in seconds; V , the orbital speed in [m/s]; G , the gravitational

constant, approximately 6.673×10^{-11} [$\text{m}^3/\text{kg}^1/\text{s}^2$]; M , the mass of Earth, approximately 5.98×10^{24} [kg].

Unless otherwise stated, the simulation environments and parameters are as follows: each RA opportunity is opened in every $\tau = \tau_s + \tau_d = 100$ [ms]; the RA signaling duration and data transmission duration are set as $\tau_s = 10$ [ms] and $\tau_d = 90$ [ms], respectively; data transmission is conducted for τ_d time only if the attempt of the access succeeds; the objective function in our MDP model corresponds to the un-discounted accumulated rewards with $\rho = 1$ over an episode up to $N = \frac{T}{T\tau} = 2604$, which corresponds to the RA opportunity; and $J = 5$ five UT agents are considered wherein two orbital planes $K = 2$ circulate over UTs with resources $P = 2$, given the MADRL environment mentioned above.

Throughout this section, we consider two benchmark RA schemes and our proposed eRACH with or without cooperation among agents as listed below.

- 1) **Slotted ALOHA** is a traditional contention-based channel access protocol. UTs agree upon the discrete slot boundaries. At the beginning of the access slot, i.e., τ_s , each UT uniform-randomly chooses the SAT to access. For each SAT, if more than one UT attempts to access at the beginning of a slot, collisions occur.
- 2) **RACH** is another conventional contention-based channel access protocol used in NR and LTE. RACH uniform-randomly selects a SAT to access and additionally chooses the preamble $p_j[n]$ at the beginning of the access slot, i.e., τ_s . When a collision occurs, UT waits for a uniformly distributed backoff time and again repeats the process from the beginning. Here, the back-off range follows a discrete uniform distribution as $\tau_b \sim DU(1, W\tau)$, where W is the backoff window size assumed fixed at 10. As in Release 16 of NR [40], we consider that RA signaling is done in two steps, i.e., 2-step RACH.
- 3) **eRACH-Coop** is another variant of our proposed RA scheme, in which each UT can select an optimal action while cooperatively communicating with other UT agents. Unlike eRACH where each distributed UT agent uses partially observable information, for eRACH-Coop, cooperative UT agents use the full observability through cheap-talk with other agents.

In particular, the cooperative UT agents use the network throughput as a corresponding reward by the previous access action of each agent, and the collision rate which involves all the collision information of each UT as state. The reward and state for the cooperative agent j is given by

$$r_j^C[n] = g(\sum_{j \in \mathcal{J}} R_j[n]), \quad (25)$$

$$\mathbf{s}_j^C[n] = \{\mathbf{s}_j[n], \sum_{j \in \mathcal{J}} R_j[n], \sum_{j \in \mathcal{J}} c_j[n]\}. \quad (26)$$

Here, this reward structure is used in the centralized training and decentralized execution (CTDE). During the centralized training, the centralized reward can be used to observe the throughput and the collision event of other UT agents. Note that each agent has its own Actor-Critic network and decide the optimal access action for itself

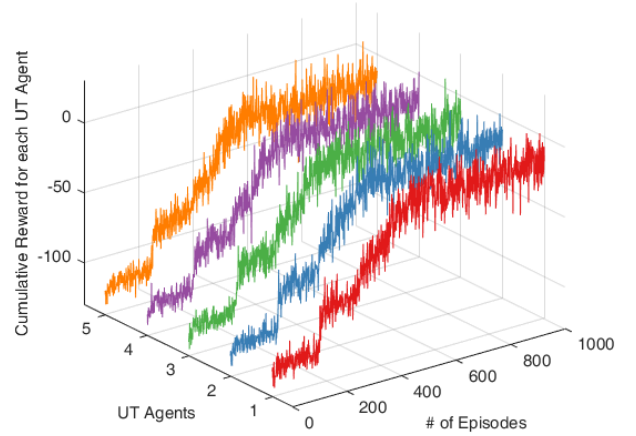


Figure 6: The convergence of eRACH for each UT agent ($J = 5$).

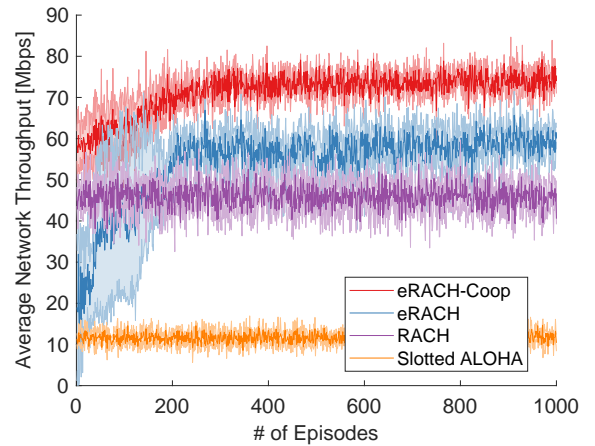


Figure 7: Network throughput for different RA schemes.

via trained policy. Here, cheap talk is necessary during both the training and exploitation phases.

- 4) **eRACH** is our proposed RA scheme with using Actor-Critic framework, wherein each UT agent optimizes its access action in the environment in a fully *distributed* manner. Each UT has partial state observability. The agents interact through the environment but do not communicate with other agents. The learning can be cast as a partially observable MDP (POMDP).

It is worth noting that in eRACH-Coop, each UT utilizes information from other UTs (see (25) and (26)) unlike the other baselines. Accordingly, eRACH-Coop can achieve better performance by using additional information. Here, one can regard its performance as an upper-bound result.

The following conditions are considered comparing the baselines: 1) all UTs have enough data to be transmitted; 2) if collisions occur at a time slot for an SAT, all attempted UTs fail to access at the time slot to the SAT; and 3) the RA signaling is done in a two step procedure (see Sec. III-B).

Table II: Throughput, collision rate, and access latency of eRACH, compared with eRACH-Coop, RACH, and Slotted ALOHA.

RA Scheme	Avg. Thr. [Mbps]	Avg. Collision Rate	Avg. Access Delay [ms]	Jain's Fairness [39]	Cheap Talk
Slotted ALOHA	12.249	0.9339	1441.1	0.8921	×
RACH	47.679	0.1338	293.1	0.9917	×
eRACH	62.347	0.6614	197.1	0.9887	×
eRACH-Coop	73.716	0.4000	151.2	0.8000	○

B. Model Architecture and Training

For all Actor and Critic NNs, we identically consider a 4-layer fully-connected multi-layer perceptron (MLP) NN architecture. Each MLP has 2 hidden layers, each of which has the 128×128 dimension with the rectified linear unit (ReLU) activation functions. Both Actor and Critic NNs are trained using RMSprop with the learning rate 0.0001, batch size 2604, 2604 iterations per episode, training episodes 1000, and 2604 iterations per update. The simulations are implemented using TensorFlow Version 2.3. Main parameters on simulation settings are summarized in Table I.

Figs. 6 and 7 plot the convergence of eRACH. Firstly, in Fig. 6, it is provided the training convergence behavior of Actor and Critic NNs for the five UT agents, in which the solid curves denote cumulative reward for each UT agent. The results show that each Actor and Critic NN for $J = 5$ converge within about 500 episodes. Besides, Fig. 7 compares eRACH and eRACH-Coop with conventional RACH and slotted ALOHA over the number of training episodes, in which shaded areas correspond to the maximum deviations during 5 simulation runs. Note that our cumulative reward corresponds to the average network throughput, such that we can validate the convergence of the proposed Actor-Critic MADRL-based method in Algorithm 1 with this figure.

As identified in this figure, eRACH and eRACH-Coop converge and outperform the conventional RACH scheme only within around 200 training episodes. It suggests that the observed data during only one day is enough to train the eRACH UT agent.

C. RA Performance Analysis

Fig. 7 and Table II compare eRACH with other baselines, in terms of network throughput, collision rate, and access delay. The results validate that eRACH achieves higher average network throughput with lower average access delay than the baselines. In particular, compared to RACH, eRACH and eRACH-Coop achieve 31.18 % and 54.61 % higher average network throughput, which is equivalent to 5.08x and 6.02x higher average network throughput of slotted ALOHA, respectively. Moreover, the results show that eRACH achieves 1.49x and 7.31x lower average access latency compared to RACH and slotted ALOHA, respectively.

Next, in terms of RA collision, the average collision rate of eRACH is 1.41x lower than slotted ALOHA, yet is 4.94x higher than RACH. As opposed to other model-based protocols, eRACH is willing to risk collisions for yielding higher throughput and lower access latency in a given network and channel environment. This fact suggests that eRACH

optimizes access flexibly according to the importance of throughput-collision in the LEO SAT network. Such flexibility is advantageous to best-effort services such as enhanced mobile broadband (eMBB) applications, but becomes a downside for mission-critical applications such as ultra-reliable and low-latency communication (URLLC). For the latter case, investigating the emergent protocols that strictly abide by a collision constraint are interesting and deferred to future work.

Lastly, comparing the performance between eRACH and eRACH-Coop in Table II, we conclude that eRACH is a fairer protocol that achieves 1.24x higher Jain's fairness than that of eRACH-Coop. The rationale is because the fully distributed operations of eRACH inherently hide the information that may promote selfish actions. Meanwhile, there is also a room to improve the fairness of eRACH-Coop by applying a fairness-aware reward function during training and/or learning fairness-aware representations for cheap talk communication, which could be an interesting direction for future research.

D. SAT Association and RA Operations

As shown in Table III, eRACH efficiently utilizes resources by optimizing the association of SAT-UT while considering the non-stationary LEO SAT network. Besides, as shown in Fig. 8, eRACH backs off flexibly thereby avoiding the collision under consideration of the given local environment, whereas when collision occurs, RACH backs off more than necessary due to a randomly selected backoff window.

In particular, eRACH-Coop in Fig. 8c shows that a certain UT agent continuously backs off. Here, since the cooperative UT agents consider the network throughput rather than the throughput of itself in the reward function, the sacrifice by this certain agent is reasonable. In contrast, for eRACH in Fig. 8b, each agent takes turns and decides to backoff. The distributed UT agents also learn how to sacrifice for the entire network even without exchanging information between agents. It suggests that the distributed eRACH protocol is able to emerge from a given local environment during the training process.

We, however, are aware of a few limitations of eRACH and eRACH-Coop, which are marked by a dotted purple line in Figs. 8b and 8c. In eRACH and eRACH-Coop, there are unnecessary backoff decisions that seem to be throughput-wise inefficient. It underlines that 1) DRL-based method occasionally decides a poor action, especially when dealing with time-series data, like our environment, and 2) the fairness issue can arise in Cooperative, during the certain agent sacrifice for the sake of the entire network.

Despite the few limitations, we observe from such comparison results that eRACH can emerge from a local environment

Table III: Top-view snapshots of SAT BS associations and preamble resource utilization (Resource Util.) under eRACH and RACH for 4 consecutive time slots, where associated and backed-off UTs are drawn with or without solid lines, respectively ($K = 2, I = 22, J = 5, P = 2$). For the same period, the RA snapshots are illustrated in Fig. 8.

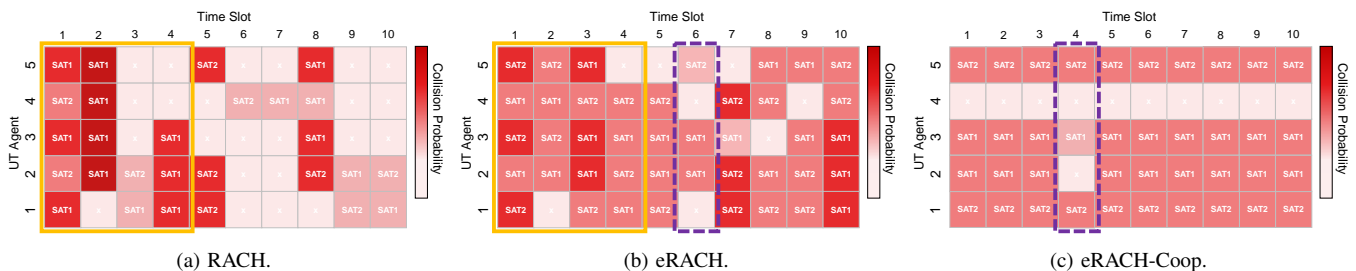
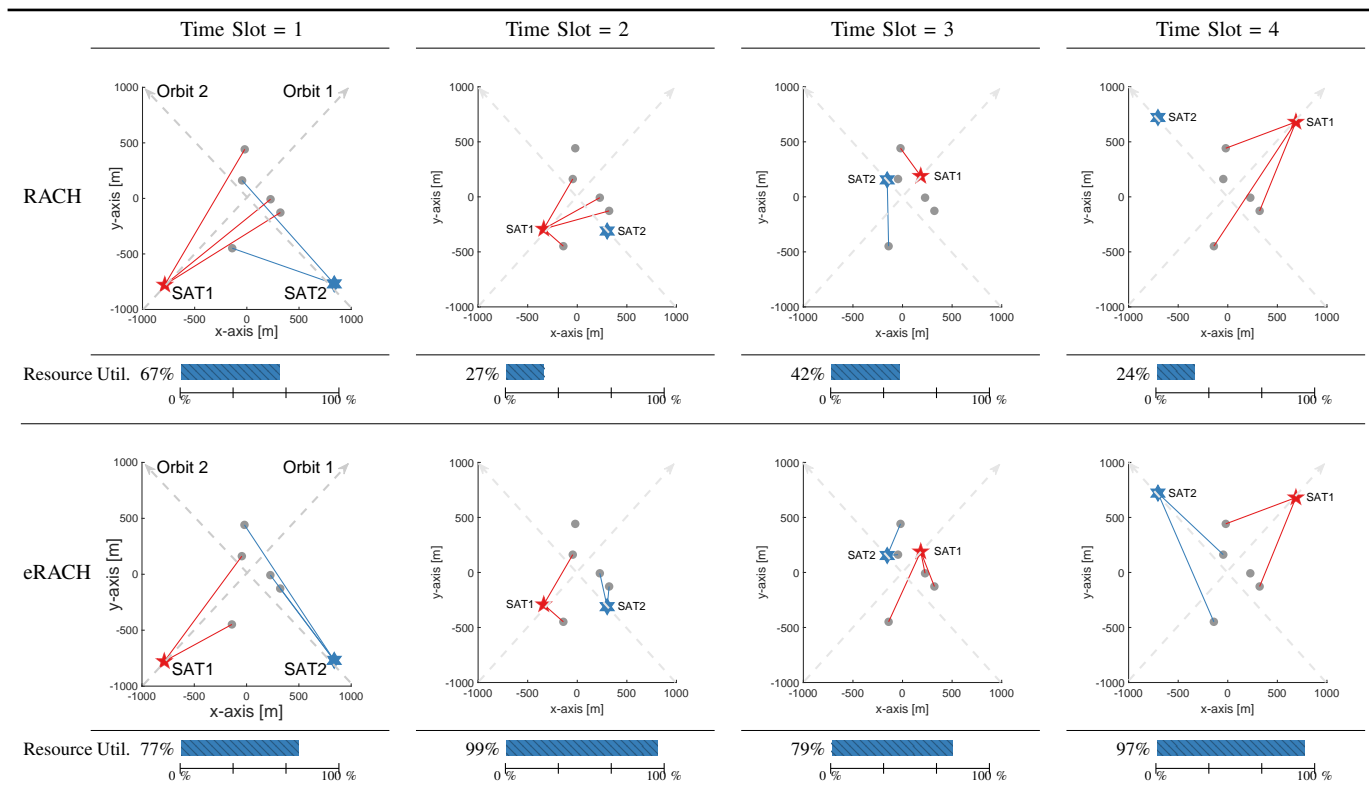


Figure 8: RA snapshots under eRACH, eRACH-Coop, and RACH for 10 consecutive time slots, where $\{\text{SAT1}, \text{SAT2}\}$ identifies SAT BS associations, and the red color of each box indicates the collision rate (the darker, the higher). For the first 4 consecutive time slots in (a) and (b), the SAT BS association snapshots are illustrated in Fig. III ($K = 2, I = 22, J = 5, P = 2$).

with the following remarkable features: 1) eRACH flexibly avoids unnecessary backoff with an understanding of the given network conditions, and 2) eRACH access the optimal LEO SAT considering the periodicity of the LEO SAT constellation.

E. Ablation Study of Key Hyper Parameters

Impact of SAT Location Precision. While training eRACH, the information of SAT location affects dominantly the reward and convergence, as explained in Fig. 4 of Sec. IV-B. However, it is challenging to find the SAT location precisely. In this regard, to examine whether easy-to-acquire prior information can be used instead of actual observed information, we present Fig. 9 and Table IV.

Specifically, various physical forces perturb SAT, e.g., Earth oblateness, solar and lunar gravitational effects, and gravita-

Table IV: Impact of SAT location precision on normalized reward and the number episodes until convergence. This table is also visualized in Fig. 5.

Position. Err.	Norm. Reward	# of Ep. for Convergence
$\sigma^2 \approx 0$	0	≈ 200
$\sigma^2 < 10^2$	0	< 300
$10^2 < \sigma^2 < 10^3$	< -5	< 700
$10^3 < \sigma^2 < 10^4$	< -45	< 2000
$\sigma^2 > 10^4$	Diverge	Diverge

tional resonance effects [29]. In actual SAT communication systems, various methods are used to track the location of perturbed SAT, such as pointing, acquisition, and tracking (PAT) mechanism [41] and global navigation satellite system (GNSS). Even with the tracking and navigation systems, some

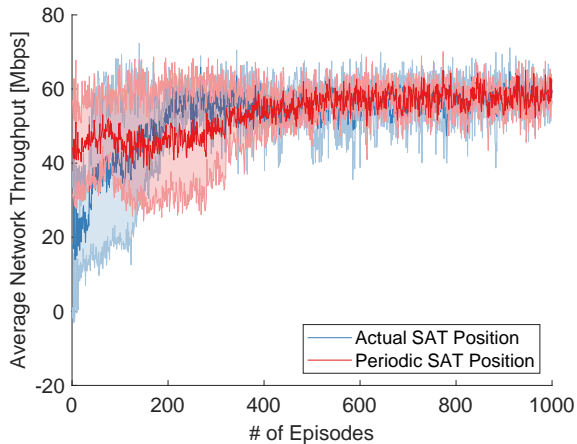


Figure 9: Impact of SAT location precision on average network throughput ($\sigma^2 = 100$).

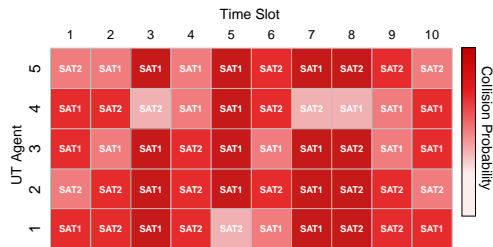
orbital positioning error of LEO SAT is inevitable. In this regard, we demonstrate the validity of the LEO SAT periodic location information, which is prior knowledge, in eRACH in Fig. 9 and Table IV.

As shown in Fig. 9, eRACH trained with the periodic LEO SAT position information converges within around 600 episodes. It closely approaches the one trained with actual LEO SAT position information. However, the periodic SAT position is not always effective for training eRACH, as shown in Table IV. The number of episodes for convergence, which corresponds to the training time, increases as the positional error goes. Besides, the overall reward decreases as the positional error goes. Nevertheless, information of periodic SAT position can still be used effectively for eRACH until the divergence point at around $\sigma^2 = 10^4$. These results suggest that eRACH can be sufficiently trained with only prior information, and this emphasize that eRACH can be trained by not only online RL but also offline RL [42].

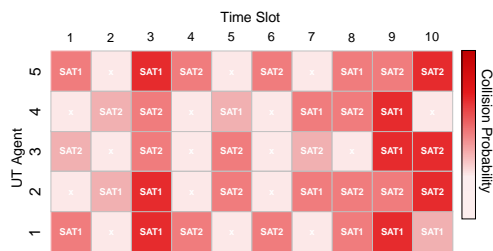
Impact of UT Distribution. The performance of the access protocol depends not only on the available resources and the number of UTs which attempt to access but also on the deployment scenario, e.g., sparse and dense networks. In this regard, we present Fig. 10 to demonstrate the impact of UT distribution on eRACH.

In the sparse networks, each UT experiences different channel conditions for SAT; thus, each UT has a particular advantageous SAT to connect to. Here, eRACH mainly focuses on designing the optimal association with SAT rather than backoff action. Whilst, in the dense networks, the channel difference between each UT is not noticeable since the distance between UTs is relatively close compared to the distance between SAT and UTs.

For the sparse case of Fig. 10a, eRACH does not backoff during the entire time slot. In contrast, in the dense case of Fig. 10b, eRACH backoff up to about 30 % of the total time slot and focuses on backoff action rather than optimal association. Notably, eRACH in both cases achieves similar performance even though they chose different aspects of access action. This

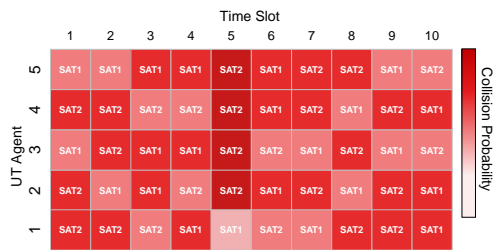


(a) Sparse Case, $d_{j,j'} = 1000$.

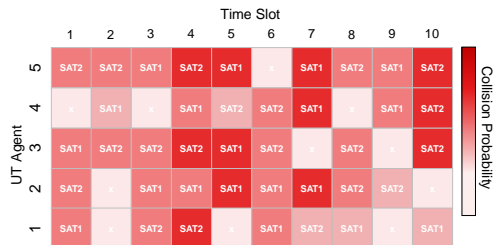


(b) Dense Case, $d_{j,j'} = 10$.

Figure 10: Impact of UT distribution on access action policy of eRACH. Here, $d_{j,j'}$ represents the average distance between UTs in [m].



(a) Rate-Max ($\rho = 0$).



(b) Collision-Aware ($\rho = 2$).

Figure 11: Impact of the collision aversion factor ρ on access action policy of eRACH.

fact further corroborates that eRACH, which flexibly decides the access action, can emerge from a given local network scenario without communication between agents.

Impact of the Collision Aversion Factor ρ . In the LEO SAT network, which suffers from a long one-way propagation delay, the contention resolution is challenging, as discussed in Sec. II. Hence, consideration for collision can be another significant issue. Regarding this, we further present the numerical results of the collision aversion case.

To clearly see the collision aversion case, we additionally

Table V: Impact of ρ on average network throughput and average collision rate of eRACH ($K = 2, I = 22, J = 5, P = 2$).

Objective	Avg. Thr. [Mbps]	Avg. Collision Rate
<i>Rate-Max</i> ($\rho = 0$)	66.391	0.6713
<i>Collision-Aware</i> ($\rho = 2$)	54.285	0.4020

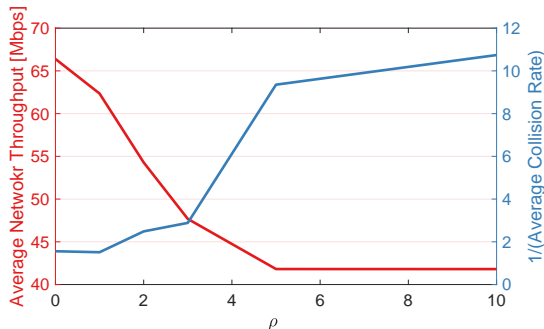


Figure 12: Comparison of eRACH over the collision aversion factor ρ .

present *Rate Max*, which only considers the throughput while training of eRACH by setting $\rho = 0$. Here, the reward function in (20) is rewritten for *Rate Max* case as follows.

$$r_j[n] = g(R_j[n]), \forall j, n. \quad (27)$$

As shown in Table V and Figs. 11 and 12, the eRACH agent learns mainly maximizing throughput or mainly minimizing collision, depending on the collision aversion factor ρ . Those results verify that eRACH method can be flexibly applied to various applications.

VI. CONCLUSION

In this article, we proposed a novel RA for LEO SAT networks. To cope with the challenges incurred by its wide coverage and time-varying network topology, we proposed a model-free RA protocol that emerges from the given LEO SAT network environment via MADRL, dubbed eRACH. By simulations, we validated that eRACH better reflects the time-varying network topology than model-based ALOHA and RACH baselines, thereby achieving higher average network throughput with lower collision rates. Furthermore, eRACH is robust to SAT BS positioning errors, enabling its operations with known periodic patterns of SAT BS locations. Lastly, eRACH can flexibly adjust and optimize throughput-collision objectives in various user population scenarios. Extending the current throughput and collision objectives, considering a fairness-aware objective could be an interesting topic for future research. It is also worth investigating highly scalable MADRL frameworks to address complicated scenarios with more orbital lanes and users at different altitudes, such as high altitude platform systems (HAPS) and other GEO and MEO SATs.

REFERENCES

- [1] N. Saeed, A. Elzanaty, H. Almorad, H. Dahrouj, T. Y. Al-Naffouri, and M.-S. Alouini, "CubeSat communications: Recent advances and future challenges," *IEEE Commun. Surveys Tuts.*, vol. 22, no. 3, pp. 1839–1862, 2020.
- [2] M. Handley, "Delay is not an option: Low latency routing in space," in *Proc. ACM Workshop on Hot Topics in Networks*, 2018, pp. 85–91.
- [3] Starlink, Accessed: Sep- 2021. [Online]. Available: <https://www.starlink.com/>
- [4] N. Pachler, I. del Portillo, E. F. Crawley, and B. G. Cameron, "An updated comparison of four low earth orbit satellite constellation systems to provide global broadband," in *Proc. IEEE International Conf. on Commun. Workshops (ICC Wkshps)*, 2021, pp. 1–7.
- [5] Federal Communication Commission (FCC). (2020, Jul.) FCC authorizes kuiper satellite constellation. [Online]. Available: <https://www.fcc.gov/document/fcc-authorizes-kuiper-satellite-constellation>
- [6] O. Kodheli, E. Lagunas, N. Maturo, S. K. Sharma, B. Shankar, J. F. M. Montoya, J. C. M. Duncan, D. Spano, S. Chatzinotas, S. Kisseleff, J. Querol, L. Lei, T. X. Vu, and G. Goussetis, "Satellite communications in the new space era: A survey and future challenges," *IEEE Commun. Surveys Tuts.*, vol. 23, no. 1, pp. 70–109, 2021.
- [7] M. Giordani and M. Zorzi, "Non-Terrestrial networks in the 6G era: Challenges and opportunities," *IEEE Network*, vol. 35, no. 2, pp. 244–251, 2021.
- [8] M. Mozaffari, W. Saad, M. Bennis, Y. Nam, and M. Debbah, "A tutorial on UAVs for wireless networks: Applications, challenges and open problems," *IEEE Commun. Surveys Tuts.*, vol. 21, no. 3, pp. 2334–2360, Mar. 2019.
- [9] Y. Zeng, R. Zhang, and T. J. Lim, "Wireless communications with unmanned aerial vehicles: Opportunities and challenges," *IEEE Commun. Mag.*, vol. 54, no. 5, pp. 36–42, May. 2016.
- [10] E. Yaacoub and M. Alouini, "A key 6G challenge and Opportunity—Connecting the base of the pyramid: A survey on rural connectivity," *Proceedings of the IEEE*, vol. 108, no. 4, pp. 533–582, Apr. 2020.
- [11] N. Saeed, H. Almorad, H. Dahrouj, T. Y. Al-Naffouri, J. S. Shamma, and M.-S. Alouini, "Point-to-Point communication in integrated Satellite-Aerial 6G networks: State-of-the-Art and future challenges," *IEEE Open J. Commun. Soc.*, vol. 2, pp. 1505–1525, 2021.
- [12] J. Foerster, Y. Assael, N. de Freitas, and S. Whiteson, "Learning to communicate with deep multi-agent reinforcement learning," in *Proc. of International Conf. on Neural Information Processing (NIPS)*, 2016, pp. 2145–2153.
- [13] A. Valcarce and J. Hoydis, "Towards joint learning of optimal MAC signaling and wireless channel access," *arXiv: 2007.09948 [cs.IT]*, 2021.
- [14] M. P. Mota, A. Valcarce, J.-M. Gorce, and J. Hoydis, "The emergence of wireless MAC protocols with Multi-Agent reinforcement learning," *arXiv: 2108.07144 [cs.IT]*, 2021.
- [15] R. De Gaudenzi and O. del Rio Herrero, "Advances in random access protocols for satellite networks," in *International Workshop on Satellite and Space Communications*, 2009, pp. 331–336.
- [16] G. Choudhury and S. Rappaport, "Diversity ALOHA - a random access scheme for satellite communications," *IEEE Trans. Wireless Commun.*, vol. 31, no. 3, pp. 450–457, 1983.
- [17] E. Casini, R. De Gaudenzi, and O. Del Rio Herrero, "Contention resolution diversity slotted aloha (CRDSA): An enhanced random access scheme for satellite access packet networks," *IEEE Trans. Wireless Commun.*, vol. 6, no. 4, pp. 1408–1419, 2007.
- [18] 3GPP TR38.811 v15.4.0, "Study on new radio (NR) to support non-terrestrial networks," Oct. 2020.
- [19] J.-H. Lee, J. Park, M. Bennis, and Y.-C. Ko, "Integrating LEO satellite and UAV relaying via reinforcement learning for Non-Terrestrial networks," in *Proc. IEEE Global Commun. Conf. (GLOBECOM)*, Taipei, Taiwan, 2020, pp. 1–6.
- [20] 3GPP TS 38.321 v16.5.0, "NR; medium access control (MAC) protocol specification," Jul. 2021.
- [21] H. Seo, J.-P. Hong, and W. Choi, "Low latency random access for sporadic MTC devices in internet of things," *IEEE Internet of Things J.*, vol. 6, no. 3, pp. 5108–5118, 2019.
- [22] 3GPP TS 38.211 v15.9.0, "NR; physical channels and modulation," Jun. 2021.
- [23] 3GPP TS 38.213 v15.14.0, "NR; physical layer procedures for control," Jun. 2021.
- [24] V. Mnih, A. P. Badia, M. Mirza, A. Graves, T. Lillicrap, T. Harley, D. Silver, and K. Kavukcuoglu, "Asynchronous methods for deep reinforcement learning," in *Proc. of International Conf. on Machine Learning (ICML)*, vol. 48, New York, New York, USA, 20–22 Jun 2016, pp. 1928–1937.
- [25] V. Mnih, K. Kavukcuoglu, D. Silver, and et al., "Human-level control through deep reinforcement learning," *Nature*, vol. 518, pp. 529–533, 2015.

- [26] D. Silver, G. Lever, N. Heess, T. Degris, D. Wierstra, and M. Riedmiller, "Deterministic policy gradient algorithms," ser. Proc. of International Conf. on Machine Learning (ICML), 2014, p. 387–395.
- [27] J. Foerster, G. Farquhar, T. Afouras, N. Nardelli, and S. Whiteson, "Counterfactual Multi-Agent policy gradients," in *AAAI Conf. on Artificial Intelligence*, 2018.
- [28] Y. Zeng and R. Zhang, "Energy-efficient UAV communication with trajectory optimization," *IEEE Trans. Wireless Commun.*, vol. 16, no. 6, pp. 3747–3760, Jun. 2017.
- [29] H. Yoon, *Pointing system performance analysis for optical inter-satellite communication on CubeSats*. Massachusetts Institute of Technology (MIT), 2017.
- [30] A. Al-Hourani and I. Guvenc, "On modeling Satellite-to-Ground Path-Loss in urban environments," *IEEE Commun. Lett.*, vol. 25, no. 3, pp. 696–700, 2021.
- [31] C. Zhan and Y. Zeng, "Energy-efficient data uploading for cellular-connected UAV systems," *IEEE Trans. Wireless Commun.*, vol. 19, no. 11, pp. 7279–7292, 2020.
- [32] Y. Zeng, J. Xu, and R. Zhang, "Energy minimization for wireless communication with rotary-wing UAV," *IEEE Trans. Wireless Commun.*, vol. 18, no. 4, pp. 2329–2345, Apr. 2019.
- [33] J.-H. Lee, K.-H. Park, Y.-C. Ko, and M.-S. Alouini, "Throughput maximization of mixed FSO/RF UAV-aided mobile relaying with a buffer," *IEEE Trans. Wireless Commun.*, vol. 20, no. 1, pp. 683–694, 2021.
- [34] —, "Optimal resource allocation and placement for terrestrial and aerial base stations in mixed RF/FSO backhaul networks," in *Proc. IEEE Vehicular Technology Conf. (VTC-Spring)*, May 2020, pp. 1–5.
- [35] J. Foerster, N. Nardelli, G. Farquhar, T. Afouras, P. H. S. Torr, P. Kohli, and S. Whiteson, "Stabilising experience replay for deep Multi-Agent reinforcement learning," ser. Proc. of International Conf. on Machine Learning (ICML), vol. 70, Sydney, Australia, 06–11 Aug 2017, pp. 1146–1155.
- [36] H. van Hasselt, A. Guez, M. Hessel, V. Mnih, and D. Silver, "Learning values across many orders of magnitude," 2016, p. 4294–4302.
- [37] V. R. Konda and J. N. Tsitsiklis, "Actor-critic algorithms," ser. Proc. of International Conf. on Neural Information Processing (NIPS), 1999, pp. 1008–1014.
- [38] Z. Wang, V. Bapst, N. Heess, V. Mnih, R. Munos, K. Kavukcuoglu, and N. de Freitas, "Sample efficient actor-critic with experience replay," *arXiv: 1611.01224 [cs.LG]*, 2017.
- [39] J. Mo and J. Walrand, "Fair end-to-end window-based congestion control," *IEEE/ACM Transactions on Networking*, vol. 8, no. 5, pp. 556–567, 2000.
- [40] 3GPP TR 21.916 v0.5.0, "Release 16 description; summary of rel-16 work items," Sep. 2021.
- [41] M. Scheinfeild, N. S. Kopeika, and R. Melamed, "Acquisition system for microsatellites laser communication in space," in *Free-Space Laser Communication Technologies XII*, vol. 3932. SPIE, 2000, pp. 166 – 175.
- [42] J. Schrittwieser, T. Hubert, A. Mandhane, M. Barekatin, I. Antonoglou, and D. Silver, "Online and offline reinforcement learning by planning with a learned model," *arXiv: 2104.06294 [cs.LG]*, 2021.